

Article

β -Carboline Alkaloids from *Peganum harmala* Inhibit *Fusarium oxysporum* from *Codonopsis radix* through Damaging the Cell Membrane and Inducing ROS Accumulation

Zihao Zhu ^{1,2}, Shujuan Zhao ^{1,2,*} and Changhong Wang ^{1,2,*} 

¹ The SATCM Key Laboratory for New Resources & Quality Evaluation of Chinese Medicine, Institute of Chinese Materia Medica, Shanghai University of Traditional Chinese Medicine, Shanghai 201203, China

² The MOE Key Laboratory for Standardization of Chinese Medicines, Shanghai Key Laboratory of Compound Chinese Medicines, Shanghai University of Traditional Chinese Medicine, Shanghai 201203, China

* Correspondence: zhaoshujuan@shutcm.edu.cn (S.Z.); wchcxm@shutcm.edu.cn (C.W.)

Abstract: *Fusarium oxysporum* is a widely distributed soil-borne pathogenic fungus that can cause medicinal herbs and crops to wither or die, resulting in great losses and threat to public health. Due to the emergence of drug-resistance and the decline of the efficacy of antifungal pesticides, there is an urgent need for safe, environmentally friendly, and effective fungicides to control this fungus. Plant-derived natural products are such potential pesticides. Extracts from seeds of *Peganum harmala* have shown antifungal effects on *F. oxysporum* but their antifungal mechanism is unclear. In vitro antifungal experiments showed that the total alkaloids extract and all five β -carboline alkaloids (β Cs), harmine, harmaline, harmane, harmalol, and harmol, from *P. harmala* seeds inhibited the growth of *F. oxysporum*. Among these β Cs, harmane had the best antifungal activity with IC₅₀ of 0.050 mg/mL and MIC of 40 μ g/mL. Scanning electron microscopy (SEM) and transmission electron microscopy (TEM) results revealed that the mycelia and spores of *F. oxysporum* were morphologically deformed and the integrity of cell membranes was disrupted after exposure to harmane. In addition, fluorescence microscopy results suggested that harmane induced the accumulation of ROS and increased the cell death rate. Transcriptomic analysis showed that the most differentially expressed genes (DEGs) of *F. oxysporum* treated with harmane were enriched in catalytic activity, integral component of membrane, intrinsic component of membrane, and peroxisome, indicating that harmane inhibits *F. oxysporum* growth possibly through damaging cell membrane and ROS accumulation via regulating steroid biosynthesis and the peroxisome pathway. The findings provide useful insights into the molecular mechanisms of β Cs of *P. harmala* seeds against *F. oxysporum* and a reference for understanding the application of β Cs against *F. oxysporum* in medicinal herbs and crops.

Keywords: *Fusarium oxysporum*; antifungal; *Peganum harmala*; β -carboline alkaloids; harmane; transcriptome



Citation: Zhu, Z.; Zhao, S.; Wang, C. β -Carboline Alkaloids from *Peganum harmala* Inhibit *Fusarium oxysporum* from *Codonopsis radix* through Damaging the Cell Membrane and Inducing ROS Accumulation. *Pathogens* **2022**, *11*, 1341. <https://doi.org/10.3390/pathogens11111341>

Academic Editor: László Kredics

Received: 4 October 2022

Accepted: 10 November 2022

Published: 13 November 2022

Publisher's Note: MDPI stays neutral with regard to jurisdictional claims in published maps and institutional affiliations.



Copyright: © 2022 by the authors. Licensee MDPI, Basel, Switzerland. This article is an open access article distributed under the terms and conditions of the Creative Commons Attribution (CC BY) license (<https://creativecommons.org/licenses/by/4.0/>).

1. Introduction

High-quality medicinal herbs are the material basis for the inheritance and development of traditional Chinese medicine and are strategic resources related to the national economy and people's livelihood. In recent years, with the growing demand for high-quality medicinal herbs at home and abroad, the species and area of artificially cultivated medicinal herbs have increased significantly [1]. However, problems such as root rot and fusarium wilt are becoming more and more serious in the process of planting medicinal herbs, such as *Panax ginseng* [2], *Codonopsis radix* [3], *Panax quinquefolius* [4], and *Crocus sativus* [5], resulting in the decline of yield and quality of medicinal herbs [6]. *Fusarium oxysporum*, a widely distributed soil-borne pathogenic fungus with strong destructiveness, is the main pathogen causing root rot or fusarium wilt of the medicinal plants [7]. It can infect more than 150 crops, such as banana, tomato, soybean, and wheat before harvest [8–10],

and it was listed as one of the top ten plant pathogenic fungi in the world in 2012 [11]. A recent prediction showed that the banana wilt caused by *F. oxysporum* worldwide would cause economic losses of more than 10 billion dollars by 2040 [12].

In addition, *F. oxysporum* can produce some secondary metabolites in the process of infection of crops, such as fusaric acid, fumonisins, and beauvericin [13,14]. These toxins may cause nausea, diarrhea, dizziness, fever and food-poisoning leukopenia, which pose a potential threat to livestock [15] and human health [16].

At present, chemical antimicrobial agents, such as azoxystrobin and thiophanate methyl, are often used to prevent and treat plant diseases caused by agriculture fungal pollution [17,18]. Azoxystrobin is a broad-spectrum fungicide with good activity against almost all fungal diseases and it is the best-selling fungicide in the world. However, long-term heavy use of such chemicals would cause drug resistance of pathogenic fungi, pollutes the environment, and has potential food safety risks, threatening human health, which does not meet the needs of the sustainable development of modern agriculture [19]. Therefore, it is urgent to develop green, safe and effective natural antimicrobial agents to control soil-borne diseases caused by *F. oxysporum*.

Many natural plant active compounds have attracted much attention due to their excellent antimicrobial activities, such as chlorogenic acid [20], allicin [21], eugenol [22], and curcumin [23]. *Peganum harmala*, a perennial herb from the Zygophyllaceae family, is widely distributed in arid grasslands in desert areas, lightly salinized sandy land on the edge of oasis, loamy low hillsides or river valley dunes of Central Asia, Europe, and southern South America. It is commonly used in folk medicine to treat fever, cough, diarrhea, hypertension, asthma, jaundice, and skin diseases [24]. It is rich in β -carboline alkaloids (β Cs), the content of which in seeds reaches up to 10%, including harmine, harmaline, harmalol, harmol, and harmane (Figure 1) [25–27]. Studies have shown that extracts from seeds of *P. harmala* have broad spectrum activities against fungi, such as *F. oxysporum*, *Aspergillus niger*, *Cryptococcus neoformans*, *Alternaria* sp., and *Epidermophyton floccosum* [27,28]. However, studies on the antifungal activity of β Cs from *P. harmala* against *F. oxysporum* are limited and the antifungal mechanism has not been elucidated.

In this paper, the potential antifungal effect of β Cs, especially harmane on *F. oxysporum* was investigated. Scanning electron microscopy (SEM), transmission electron microscopy (TEM), and transcriptome analysis were conducted to explore the inhibition mechanism, which showed that harmane inhibits the mycelial growth of *F. oxysporum* possibly through regulating the expression of genes related to steroid biosynthesis and peroxisome metabolism. This study provides a reference for understanding the application of β Cs in medicinal herbs and crops.

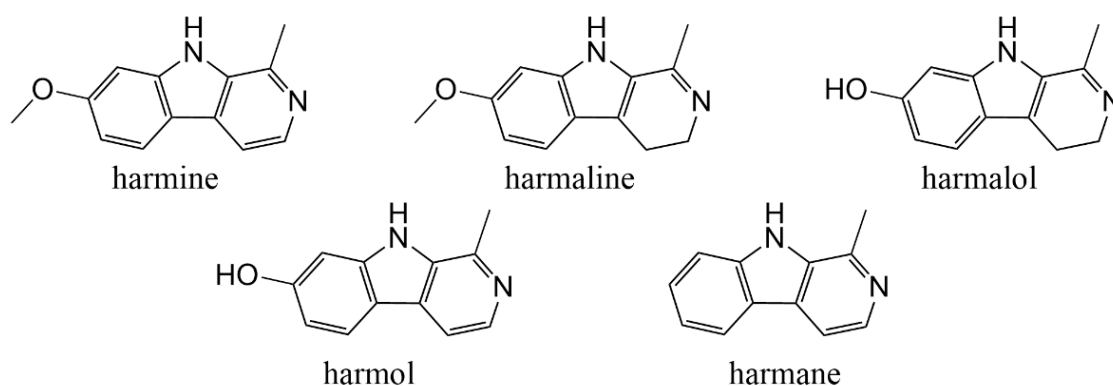


Figure 1. Structures of the five main β Cs in *P. harmala* seeds.

2. Materials and Methods

2.1. Isolation and Identification of *F. oxysporum*

F. oxysporum was isolated according to the previously reported methods [29]. Briefly, fungal pathogens were isolated from root of *Codonopsis radix* with root rot collected in Gansu province of China, and grown on potato dextrose agar (PDA). After 5 days of culturing, the colony was convex flocculent, pinkish white, slightly purple. The mycelium was white and dense. It was identified as *F. oxysporum* by morphological characteristics and 16S rRNA sequence analysis (Genbank MK966308).

Spore suspension was prepared according to the literature with slight modifications [30]. In short, the spore suspension was collected by flooding the surface of the 7-day-old culture plates with sterile water and filtering with sterile degreasing cotton. Then, the *F. oxysporum* spore suspension was diluted to a concentration of approximately 1.0×10^6 CFU/mL, using a hemocytometer.

2.2. Chemicals

Harmine (CAS NO. 442-51-3, purity 98%), harmaline (CAS NO. 304-21-2, purity 98%), harmalol (CAS NO. 525-57-5, purity 98%), harmol (CAS NO. 487-03-6, purity 98%), and harmane (CAS NO. 486-84-0, purity 98%), and total alkaloid extracts were isolated from *P. harmala* seeds by our laboratory [31]. The content of harmine and harmaline in total alkaloid extracts was 55.3%. The structures of β Cs included in the project are shown in Figure 1. Azoxystrobin (CAS NO. 131860-33-8, purity 98%) was purchased from Beijing Norma Standard Technology Co., Ltd (Beijing, China).

2.3. Inhibition of Total Alkaloids on Mycelial Growth

The inhibition effect of total alkaloid extracts from *P. harmala* seeds against *F. oxysporum* were tested by agar diffusion method [32]. Alkaloid extracts from *P. harmala* were mixed with PDA, and the final concentrations were 0.05, 0.1, 0.2, 0.4, and 0.5 mg/mL. Azoxystrobin at dose of 0.4 mg/mL was used as a positive control. *F. oxysporum* was inoculated on the PDA and cultured at 28 °C for 5 days. PDA without alkaloid was used as a control. The mycelial growth diameter of *F. oxysporum* colony was measured and the inhibition rate was calculated according to the following Formula (1).

$$\text{Inhibition rate (\%)} = \frac{\text{the diameter of control} - \text{the diameter of treatment}}{\text{the diameter of control}} \times 100\% \quad (1)$$

2.4. Inhibition of Five β Cs on Mycelial Growth and IC_{50} CALCULATION

The inhibition effect of the five β Cs on *F. oxysporum* was tested in the same way as total β Cs. The IC_{50} was analyzed using SPSS (version 25.0, Norman H. Nie, C. Hadlai (Tex) Hull and Dale H. Bent, CA, USA).

2.5. Determination of Minimal Inhibitory Concentration (MIC)

According to the American Society for Clinical and Laboratory Standards (CLSI) standard, the MIC of β Cs against *F. oxysporum* was determined by tube double dilution method in a 96-well plate [33]. β Cs were separately mixed with Potato Dextrose Broth (PDB) in the concentration range of 0.625–50 μ g/mL, and 4 mL of the mixed solution was added into 20 μ L of the conidial suspension. Then, each concentration of the mixed solution was successively distributed to three wells of the 96-well plate. PDB without β Cs was used as the control group. The MIC was defined as the lowest drug concentrations that caused complete visible inhibition of growth.

2.6. Scanning Electron Microscopy (SEM)

The morphology of *F. oxysporum* after harmane treatment was observed with SEM according to the literature [34]. The spore suspension was added into PDB and cultured at 28 °C (120 rpm) for 48 h. After centrifugation at 4000× *g* for 5 min, the mycelium was suspended again in PBS (pH 7.2). The βCs were added to the buffer solution to make the concentration MIC and incubated at 28 °C for 12 h, with anhydrous ethanol as the control group [35].

The samples were fixed in 2.5% glutaraldehyde, washed with PBS three times, 15 min each time, fixed with 1% osmic acid solution for 1 h, washed three times, 15 min each time. The samples were dehydrated with ethanol solution of five concentration gradients (including 30%, 50%, 70%, 80%, 90% and 95%). Each concentration was treated for 15 min, and then 100% ethanol was used twice, 20 min each time. The sample was treated with the mixture of ethanol and isoamyl acetate for 30 min, and then treated with pure isoamyl acetate for 1 h, dried, coated and examined by SEM (×10.0K and ×20.0K, U8010, Hitachi, Tokyo, Japan).

2.7. Transmission Electron Microscopy (TEM)

For TEM, mycelia were treated the same way as SEM and slightly modified. In short, the treated samples were fixed in 2.5% glutaraldehyde and washed three times with PBS for 15 min each time. The samples were dehydrated with ethanol solution of five concentration gradients (including 30%, 50%, 70%, 80%, 90% and 95%). Each concentration of the sample was treated for 15 min and then treated twice with 100% ethanol for 20 min each time. The samples were embedded for 3 h and sliced in an ultra-thin cutting machine (UC7, Leica, Wetzlar, Germany). The samples were stained with lead citrate solution and 50% ethanol saturated solution of uranium dioxide acetate for 5 min, respectively, and then examined by TEM (H-7650, Hitachi).

2.8. Evaluation of Release of Cell Components

The release of cell components was evaluated using OD₂₆₀ determined with UV spectrophotometry [35]. To do that, the 1 × 10⁶ CFU/mL suspension was mixed with PDB and cultured at 28 °C (120 rpm) for 48 h. After centrifugation at 4000× *g* for 15 min, the mycelia were collected and washed with sterile water three times. Then, the mycelia were suspended in phosphate buffer solution (PBS, pH 7.2), supplied with harmane at the final concentration of 0.5 MIC and MIC, then incubated at 28 °C for 4 h, 8 h, and 12 h, respectively. Samples were centrifuged at 4000× *g* for 5 min to collect supernatant for OD₂₆₀ measurement. PBS (pH 7.2) was used as the control.

2.9. Measurement of Electrical Conductivity

The influence of harmane on electrical conductivity of *F. oxysporum* was measured according to the literature [32]. The sample was treated in the same way as for cell component assay. The conductivity of the supernatant of different samples was determined using conductivity meter (DDS-11D, JingKe, Shanghai, China).

2.10. ROS Assay

The content of ROS in cells was evaluated by Reactive Oxygen Species assay kit (Beyotime, Shanghai) combined with fluorescence microscopy. The method of culture and treatment of samples was described in SEM. The DFCH-DA probe was added into the treated samples and incubated at 37 °C for 30 min. After centrifugation, the supernatant was washed twice with PBS, and the precipitation was collected and observed under bright light and green light by fluorescence microscopy (×10, Olympus IX81, Tokyo, Japan).

2.11. Annexin V-FITC/PI Double Staining Assay

The cell death rate was analyzed using Annexin V-FITC Apoptosis detection kit (Beyotime, Shanghai, China) combined with fluorescence microscopy, which could also

discriminate types of cell death (apoptotic or necrotic cell death) [30]. The method of culture and treatment of samples was described in SEM. Briefly, a total of 500 μL of the treated sample was mixed with 5 μL of Annexin V-FITC and then 5 μL of propidium iodide (PI) was added, incubated at 25 °C for 10 min, and imaged under fluorescence microscopy (Olympus IX81).

2.12. Transcriptomic Analysis

The total RNA of the treated samples was extracted with TRIzol® Reagent (Invitrogen, Carlsbad, CA, USA), according to the manufacturer's instructions, and genomic DNA was removed using DNase I (TaKara, Kyoto, Japan). Its concentration, purity and integrity were detected by Nanodrop2000 (NanoDrop Technologies, Waltham, MA, USA). The transcriptome library was prepared following Truseq™ RNA sample preparation kit from Illumina (San Diego, CA, USA) using 1 μg of total RNA. Then, the synthesized cDNA was subjected to end-repair, phosphorylation and 'A' base addition according to Illumina's library construction protocol. Libraries were size selected for cDNA target fragments of 300 bp on 2% Low Range Ultra Agarose followed by PCR amplified using Phusion DNA polymerase (NEB) for 15 PCR cycles. After quantified by TBS380, paired-end RNA-seq sequencing library was sequenced with the Illumina NovaSeq 6000 sequencer (2 × 150 bp read length). The original sequencing data was subjected to quality control using SeqPrep (<https://github.com/jstjohn/SeqPrep>, accessed on 15 November 2021) and Sickle (<https://github.com/najoshi/sickle>, accessed on 15 November 2021) software to obtain clean data. These clean data were compared with the reference genome (*Fusarium oxysporum*, http://fungi.ensembl.org/Fusarium_oxysporum/Info/Index, accessed on 15 November 2021) using HiSat2 (<http://ccb.jhu.edu/software/hisat2/index.shtml>, accessed on 15 November 2021) to obtain mapped data for subsequent transcript assembly, expression amount calculation, and others. The RSEM (<http://deweylab.biostat.wisc.edu/rsem/>, accessed on 22 November 2021) software was used to perform progressive analysis on the expression levels of genes and transcripts to obtain read counts, and DESeq2 (<http://bioconductor.org/packages/stats/bioc/DESeq2/>, accessed on 22 November 2021) software was used to identify differentially expressed genes (DEGs) between samples using $\text{FDR} < 0.05$ & $|\log_2\text{FC}| \geq 1$ as the standard. DEGs were annotated and analyzed for enrichment in the GO database (<http://www.geneontology.org>, accessed on 3 July 2022) and the KEGG database (<http://www.genome.jp/kegg/>, accessed on 3 July 2022), respectively.

2.13. Statistical Analysis

Three independent experiments were performed for each assay. All statistical analyses were performed using GraphPad Prism 9.0.0 (Harvey Moltusky, San Diego, CA, USA), and regression analysis was used to determine the significant differences with 95% confidence ($p < 0.05$).

3. Results

3.1. Inhibition of Total Alkaloid Extracts from *P. harmala* on Mycelial Growth

Results revealed that total alkaloids exhibited inhibition on mycelial growth (Figure 2A). The inhibitory effect of total alkaloids on mycelial growth was concentration-dependent. The mycelial growth inhibition rates at concentrations of 0.05, 0.1, 0.2, 0.4, and 0.5 mg/mL were 16.3%, 21.4%, 32.2%, 51.3% and 56.3%, respectively (Figure 2B). The mycelial growth inhibition rate of the positive control group at dose of 0.4 mg/mL was 84.2%. These results showed that total alkaloid extracts from *P. harmala* can inhibit the growth of *F. oxysporum*.

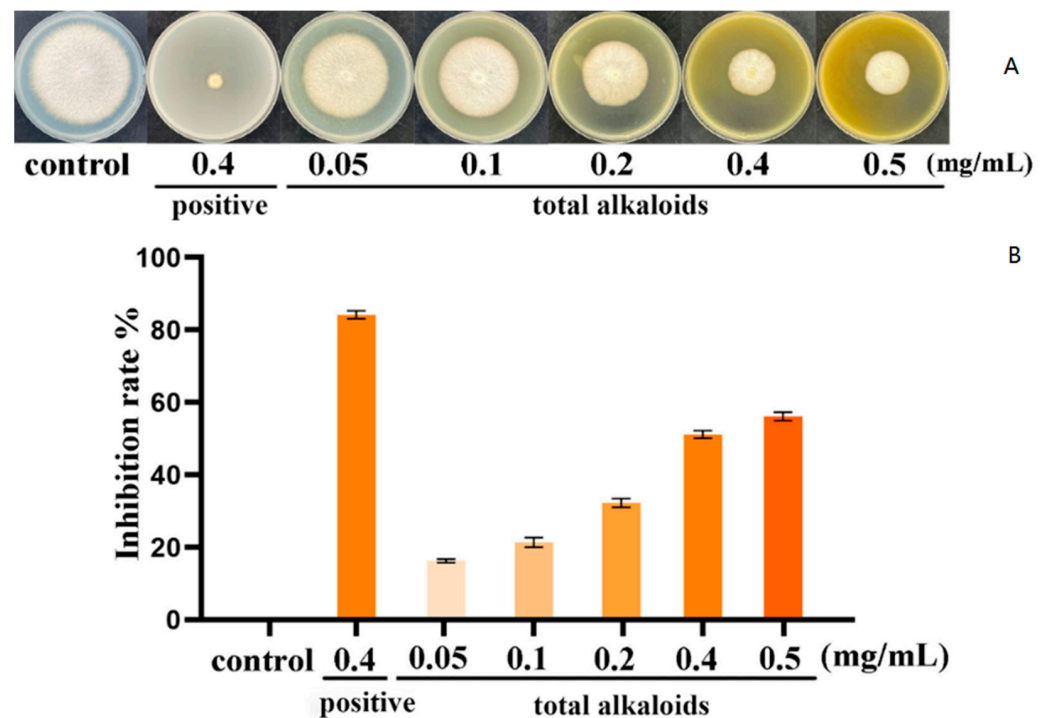


Figure 2. The inhibitory effects of total alkaloid extracts from *P. harmala* against *F. oxysporum*. (A) The inhibitory effects of total alkaloids on mycelial growth of *F. oxysporum*. (B) The inhibition rate of total alkaloids against *F. oxysporum*.

3.2. Inhibition of Five Target β Cs on Mycelial Growth

To further explore the effect of total alkaloids, five main alkaloids were cultured with *F. oxysporum*. As shown in Figure 3A, all the five β Cs had obvious inhibitory effect on *F. oxysporum* and the inhibition zone increased with the concentration of β Cs from 0.05 to 0.5 mg/mL, indicating that the antifungal effect of β Cs against *F. oxysporum* was in a concentration-dependent manner. Among the five β Cs, harmane had the most significant inhibitory effect. When the concentration was 0.5 mg/mL, the mycelia nearly stopped growing, and the inhibitory rate reached 100% (Figure 3B).

The IC_{50} of the five β Cs from low to high were 0.050 mg/mL (harmaine), 0.143 mg/mL (harmine), 0.161 mg/mL (harmol), 0.331 mg/mL (harmaline), and 0.798 mg/mL (harmalol) (Table 1). Harmaine showed the best antifungal activity and was investigated in subsequent experiments.

Table 1. IC_{50} of the five β Cs on *F. oxysporum*.

β Cs	Harmaine	Harmaline	Harmalol	Harmaine	Harmol
IC_{50} (mg/mL)	0.143	0.331	0.798	0.050	0.161

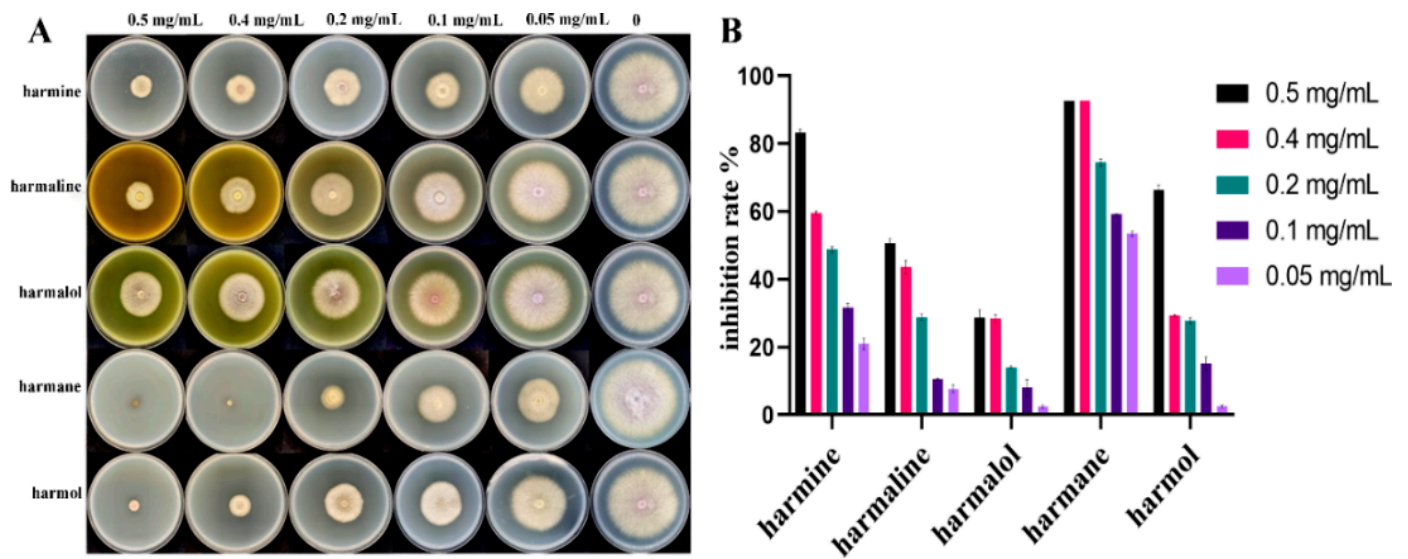


Figure 3. The inhibitory effects of the five β Cs on *F. oxysporum*. (A) The inhibitory effect of the five β Cs on mycelial growth of *F. oxysporum*. (B) The inhibition rate of five β Cs against *F. oxysporum*.

3.3. MIC

By observing the clarification of different concentrations, we found that when the concentration of harmane was 40 μ g/mL, the fungal liquid was clear, and when the concentration was 20 μ g/mL and lower, the fungal liquid was turbid. OD₆₀₀ values are shown in Figure 4. It was determined that the MIC of harmane was 40 μ g/mL.

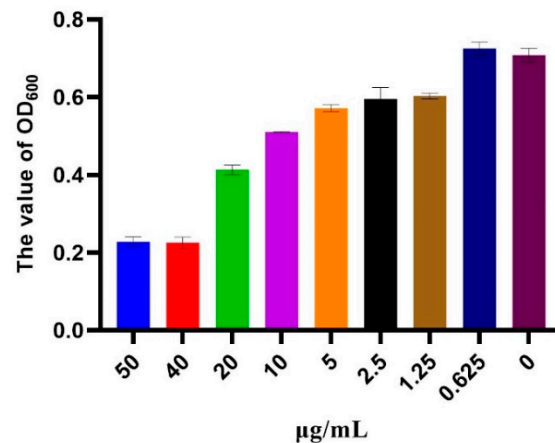


Figure 4. The value of OD₆₀₀ of *F. oxysporum* cultures with different concentrations of harmane.

3.4. SEM

The results of SEM analyses of *F. oxysporum* spores are shown in Figure 5. It can be observed that the morphology of hyphae and spores had undergone significant changes. From the control group, it can be seen that mycelia and spores are with a smooth surface and plump in shape, with no wrinkles and have a normal growth (Figure 5A,B). The surface of mycelia and spores in the treatment group was wrinkled, depressed, shriveled, and deformed where the red arrows pointed (Figure 5C,D). It can be seen that inhibition of harmane against *F. oxysporum* mainly affects cell morphology and leads to cell atrophy.

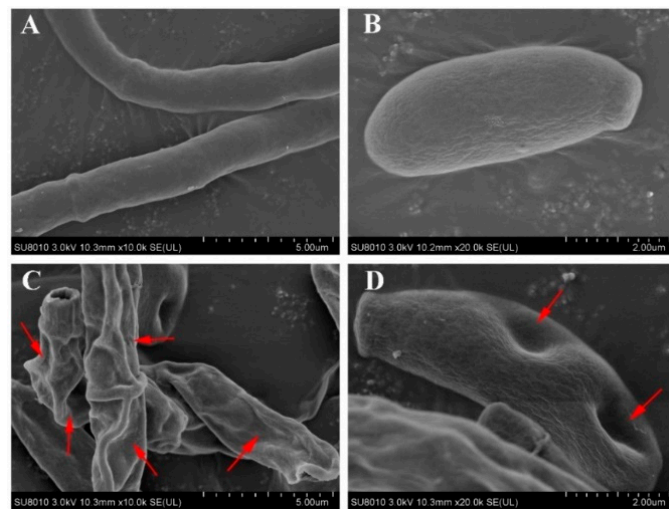


Figure 5. Morphology of *F. oxysporum* under SEM, (A,B) Morphology of normal growth of mycelia and spores in the control group, (C,D) Morphology of mycelia and spores induced by harmaline. (A,C) $\times 10K$, bar = 5.00 μm , (B,D) $\times 20K$, bar = 5.00 μm .

3.5. TEM

The ultrastructural changes of *F. oxysporum* were further observed by TEM and results are shown in Figure 6. In the control group, the cell boundary was clear, the cell wall was complete, the thickness was uniform, the cell morphology was elliptical, the organelles were arranged neatly, and the cell growth was normal (Figure 6A,B). The mycelia in the treatment group were dissolved in irregular oval shape, the integrity of cell wall was destroyed, and the cytoplasm was blurred where the red arrows pointed (Figure 6C,D). This result confirmed that the permeability or integrity of cell membrane was destroyed.

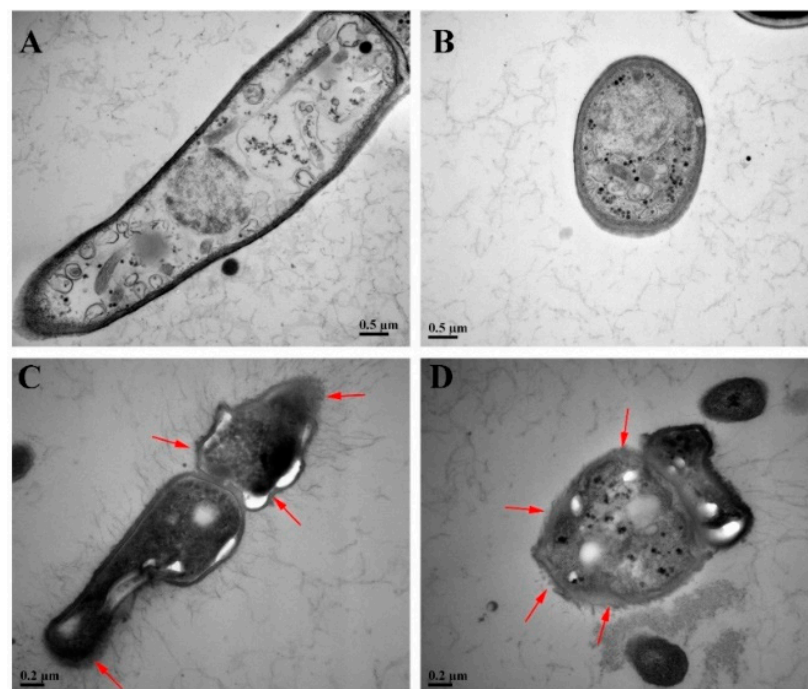


Figure 6. Ultrastructure of mycelia and spores under TEM, (A,B) Ultrastructure of mycelia and spores in the control group, (C,D) Ultrastructure of mycelia and spores induced by harmaline. (A,C) Longitudinal section through the mycelia, (B,D) Tangential section through the mycelia. (A,B) $\times 25K$, bar = 0.5 μm , (C,D) $\times 50K$, bar = 0.2 μm .

3.6. Detection of Release of Cell Components and Electrical Conductivity

As shown in Figure 7, at the concentrations of 0, 0.5 MIC, and MIC, harmane significantly increased the release of cell components of *F. oxysporum*. The OD₂₆₀ was 0.43 at the concentration of MIC after incubation for 12 h (Figure 7A), which was significantly higher than that in the control group ($p < 0.05$).

With the increase of processing time, the electrical conductivity also showed an increasing trend (Figure 7B). After 12 h, the electrical conductivity of the control group was the lowest (16.13 $\mu\text{S}/\text{cm}$), and the electrical conductivity of the MIC was highest (46.6 $\mu\text{S}/\text{cm}$) compared with that of the control, with significant differences ($p < 0.05$), indicating that harmane possibly disrupted the cell membrane of *F. oxysporum* and increased its permeability.

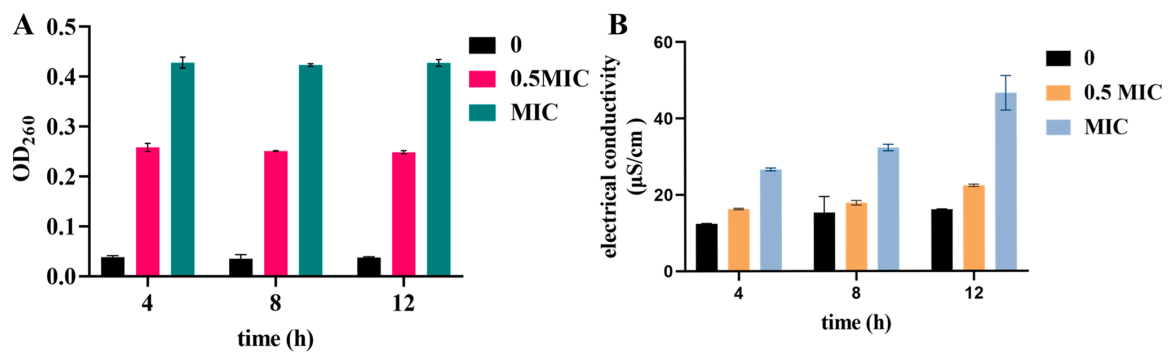


Figure 7. The effect of harmane on cellular component release and electrical conductivity of *F. oxysporum*, (A) Influence of harmane on OD₂₆₀, (B) Influence of harmane on electrical conductivity.

3.7. Harmane Induced Accumulation of ROS

DCHF-DA staining was used to evaluate the content of ROS levels in the cells after incubation with harmane. According to the literature [36], the green fluorescence brightness is positively correlated with the content of ROS in the cell. In the control group (CK), few spores with weak fluorescence were found. When the concentration of harmane was MIC, induced intracellular accumulation of ROS was noticed. The proportion of spores producing fluorescence increased in a concentration-dependent manner after treatment of harmane (Figure 8). These results suggested that harmane could cause outbreak of ROS in *F. oxysporum*.

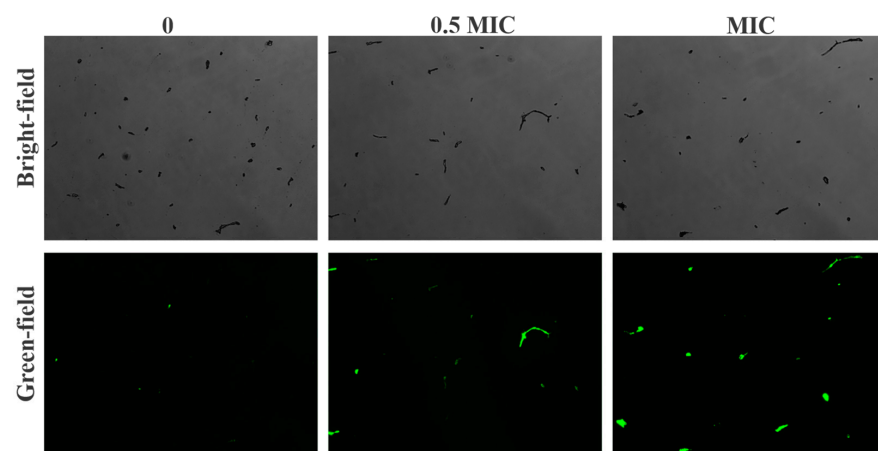


Figure 8. Harmane induced intracellular accumulation of ROS in *F. oxysporum*. Bright-field was the results of DCFH-DA staining of *F. oxysporum* under bright light ($\times 10$). Green-field was the results of DCFH-DA staining of *F. oxysporum* under green light ($\times 10$).

3.8. Cell Death Analysis

The antifungal mechanism of harmane against *F. oxysporum* was investigated using Annexin V-FITC/PI double staining. As shown in Figure 9, after Annexin V-FITC/PI staining, spores in the control group (CK) rarely show green or red fluorescence with weak fluorescence intensity. With the increase of harmane content, the green and red fluorescence intensity and percentage of the cells were higher. Most cells in the MIC group showed fluorescence, indicating that the membrane permeability of *F. oxysporum* was damaged, leading to cell death.

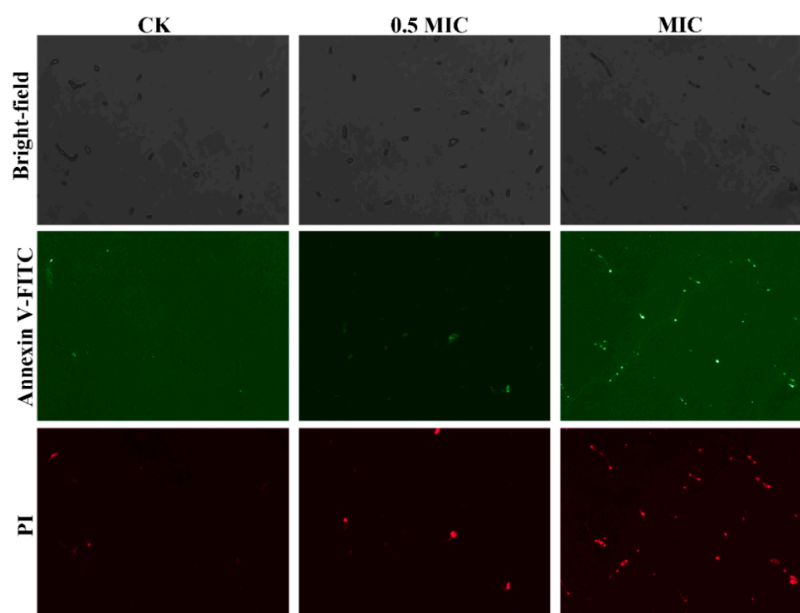


Figure 9. Harmane induced cell death of *F. oxysporum*. Annexin V-FITC was the results of Annexin V-FITC staining of *F. oxysporum* under green light ($\times 10$); PI was the results of PI staining of *F. oxysporum* under red light ($\times 10$).

3.9. Effect of Harmane on the Transcriptome of *F. oxysporum*

Transcriptome sequencing was performed to further reveal the antifungal mechanism of harmane. We collected differently treated mycelia (0, MIC) for RNA sequencing. Principal component analysis showed that the repetitions of each sample clustered together, while different groups were separated at PC1 and PC2 levels. There were significant differences in gene expression between the two groups after treatment of alkaloid. These data demonstrated that the accuracy and reliability of RNA-sequencing for later analysis. Through the analysis of the DEGs of the two groups, a total of 8624 identical genes were obtained between the control and MIC groups. A total of 300 genes were specific to the control group, and 630 genes were specific to the harmane group. After treatment of harmane, 1883 genes were differentially expressed of which 1137 genes were up-regulated and 746 genes were down-regulated. To analyze the specific differences caused by harmane, DEGs were classified according to molecular function, biological process and cellular component in GO database. Eight terms in cellular component and six terms in biological process and molecular function were affected in *F. oxysporum* under harmane treatment. Among the terms, “membrane part”, “metabolic process” and “catalytic activity” were most significantly enriched in these three categories, respectively.

Similar to the GO annotation analysis, the GO term enrichment analysis showed that DEGs related to catalytic activity, integral component of membrane and intrinsic component of membrane were the most enriched pathways (Figure 10A) in which a unigene encoding C-5 sterol desaturase (ERG3) was significantly down-regulated.

KEGG pathway enrichment analysis showed that the DEGs belonged to peroxisome pathway were the most enriched (Figure 10B) in which unigenes encoding peroxisomal

catalase (CAT) and superoxide dismutase (SOD) were significantly decreased after harmane treatment.

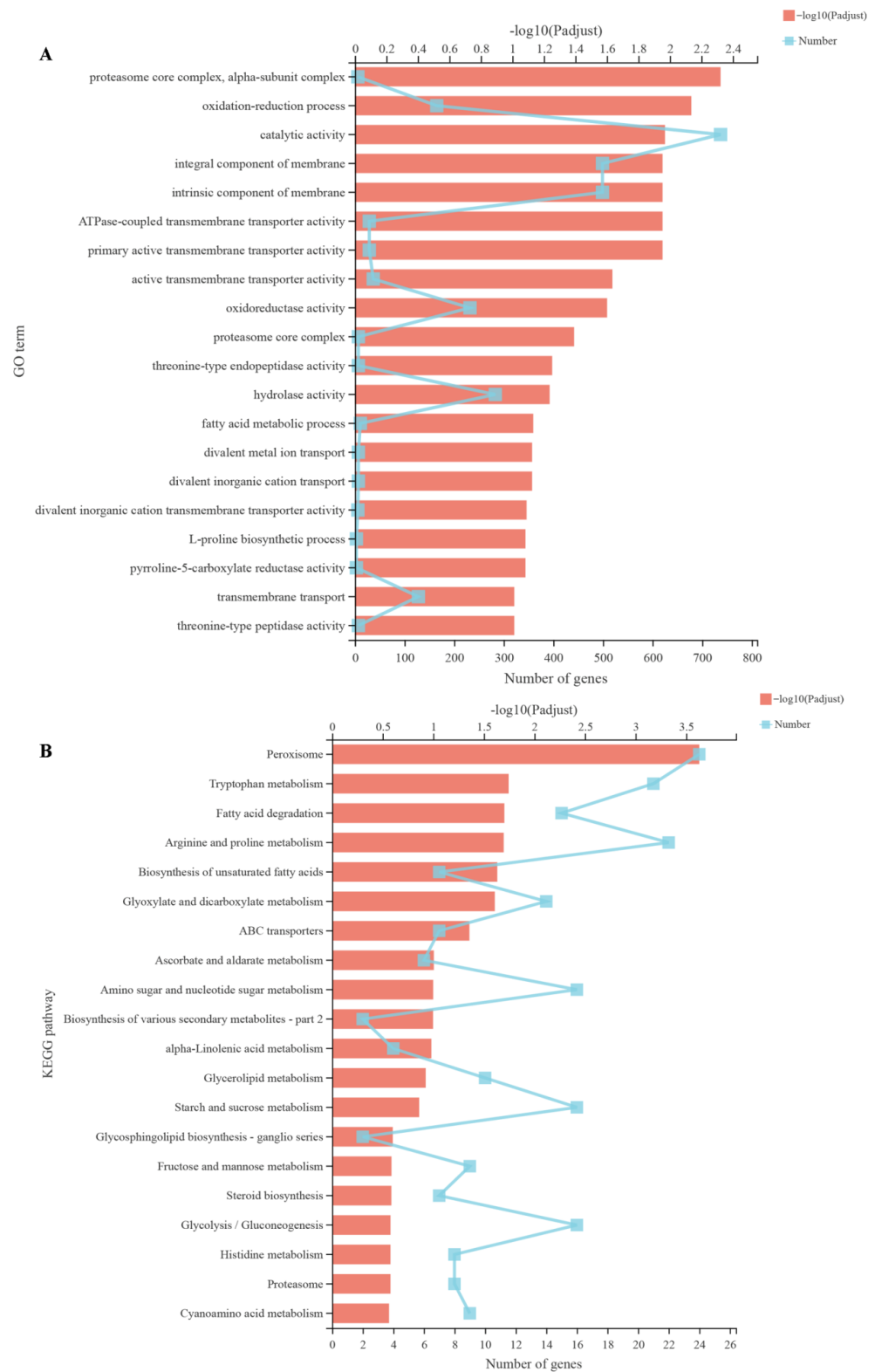


Figure 10. Cluster analysis and enrichment analysis in GO and KEGG databases, (A,B) Enrichment analysis of DEGs in GO and KEGG databases.

4. Discussion

Over the years, the long-term heavy use of pesticides has made the development of new natural antimicrobial agents with good antifungal effect more and more popular [37]. *P. harmala* is a drought tolerant plant that is widely distributed in the world [24]. Extracts from seeds of this plant have antimicrobial effects on a variety of fungi, bacteria, and viruses [27]. However, there are few in-depth studies on the antifungal activity and mechanism of the total β Cs or the five β -carboline alkaloids against *F. oxysporum*. In this study, the antifungal effect of β Cs from *P. harmala* seed extract and the mechanism of harmane against *F. oxysporum* was investigated in order to provide evidence for the development of new, green agents against *F. oxysporum*.

The mycelial growth test of the total alkaloids showed that total alkaloids had an obvious inhibitory effect on mycelial growth. This indicated that the total alkaloids were the antifungal components in the extract of *P. harmala* seed. The results of the further mycelial growth inhibition test of five β Cs showed that these β Cs from *P. harmala* extract had different degrees of inhibition on *F. oxysporum*, and harmane showed the strongest antifungal activity, with IC_{50} of 0.050 mg/mL, which was lower than that of mancozeb, hymexazol and palmatine [38,39]. The double dilution method is commonly used to measure IC_{50} in general. The inhibition rates of harmine, harmaline and harmol were with significant difference at 0.4 mg/mL and 0.5 mg/mL. Yet, there was no difference of harmane at 0.4 mg/mL and 0.5 mg/mL of which the inhibition rate was 100%. In overall consideration, we made a slight modification of tube double dilution method and chose 0.5 mg/mL for the maximum concentration.

Azoxystrobin is often used as a pesticide to prevent root rot of *C. radix* in agriculture. It is a commonly used as a positive control in the study of inhibiting *F. oxysporum* [40]. At the concentration of 0.4 mg/mL, the antifungal effect of harmane is better than that of azoxystrobin, and harmane has the potential to be developed into an antifungal drug.

The MIC of harmane was 40 μ g/mL, comparable to that of amphotericin B [41]. Harmane has the potential to be developed as a drug against *F. oxysporum*. At the same time, it is necessary to study the antifungal spectrum, which will be conducive to the development of broad-spectrum antifungal drugs. These results indicated that harmane had good antifungal potential and could be used as a potential fungicide against *F. oxysporum* in the future.

SEM and TEM results showed that after harmane treatment, the boundary of *F. oxysporum* cells was blurred; the cell membrane and cell wall are dissolved or even ruptured in some places, and the cytoplasm is disordered. It was proved that harmane damaged the cell membrane integrity of *F. oxysporum*. The increased permeability, the released cell components, and the increased extracellular electrical conductivity also supported this point.

There was no significant difference of OD_{260} at 4 h, 8 h, and 12 h, indicating that the intracellular nucleic acid was released within 4 h. The electrical conductivity was with significantly difference at 4 h, 8 h, and 12 h, indicating that the release process of a large number of sugars, proteins, nucleic acids, inorganic salts and other contents in the cells was relatively slow. Within 12 hours, their leakage increased linearly with time. This trend was consistent with previous reports [42]. OD_{260} and electrical conductivity have been proved to be important indicators of cell membrane damage [35]. Previous studies have proved that the butan-1-ol extract of *P. harmala* seeds could cause cell membrane damage [43].

β Cs could induce accumulation of ROS in plant pathogenic fungi (*Penicillium digitatum* and *Botrytis cinerea*) [44]. The fluorescence microscopy results in this study also demonstrated that harmane induced ROS accumulation in *F. oxysporum*. High concentrations of ROS can slow down cell growth and even lead to cell death through cellular oxidative stress [45,46]. Thus, the cell death detected by Annexin V-FITC/PI staining after harmane treatment was possibly partially resulted from the accumulation of ROS.

Further transcriptomic analysis revealed that harmane down-regulated the expression level of ERG3, CAT and SOD in *F. oxysporum*. ERG3, a key enzyme in the biosynthesis of

ergosterol is involved in steroid biosynthesis [47]. The disruption of ergosterol biosynthesis resulted in increased cell membrane permeability [48]. The decrease of ERG3 expression affected the growth of fungi, resulting in the inability to produce ergosterol and destruction of membrane integrity [49]. It appears that the harmane-caused damage of cell membrane of *F. oxysporum* was possibly related with the downregulation of ERG3. Cells generate ROS through a variety of pathways, which can be cleared by SOD and CAT, thereby maintaining a dynamic balance of intracellular ROS [50]. The accumulation of ROS in *F. oxysporum* caused by harmane was likely related to the reduced expression of SOD and CAT and the ROS could not be removed normally.

According to the results of cellular component release and electrical conductivity, the cell membrane damage may occur before 4 h. It would be better to verify the expression level of key unigenes earlier.

5. Conclusions

In summary, it was demonstrated that the alkaloid extract and β Cs from *P. harmala* could inhibit the mycelial growth of *F. oxysporum*. Among these β Cs, harmane had the best antifungal activity and caused damage of the morphology of mycelia and spores of *F. oxysporum*, the integrity of cell membrane, accumulation of intracellular ROS, and cell death. Combined with transcriptome analysis, harmane may disrupt the integrity of the cell membrane by regulating steroid biosynthesis and interfering with ergosterol metabolism via down-regulating genes, such as ERG3, causing cell wall dissolution and the damage of cell membrane integrity, resulting in cell death. On the other hand, harmane interferes with the metabolism of ROS by down-regulating CAT and SOD, leading to the accumulation of ROS and damage to cells, which may also cause cell death. β Cs has the potential to control *F. oxysporum* pollution as an antimicrobial agent. Therefore, future research is needed to make out the anti-*F. oxysporum* effects in fields. Our results provide important insights into the potential mechanism of β Cs inhibiting fungal growth, which may be helpful for future applications of *P. harmala* in planting medicinal herbs and crops.

Author Contributions: Z.Z. performed the experiments and drafted the manuscript. S.Z. provided technical assistance. S.Z. and C.W. designed the experiments, revised the manuscript, and provided supervision and project administration. All authors have read and agreed to the published version of the manuscript.

Funding: This research was funded by the National Key Research and Development Program of China: 2018YFC1706304; 2022YFC3501701; National Natural Science Foundation of China: 82173885; Project of Shanghai Science and Technology: 21DZ2202200; Three-year Action Plan for the Development of Traditional Chinese Medicine of Shanghai: ZY (2021-2023)-0215; Graduate Student Innovation Ability Project of Shanghai University of Traditional Chinese Medicine: Y2021004.

Institutional Review Board Statement: Not applicable.

Informed Consent Statement: Not applicable.

Data Availability Statement: Not applicable.

Conflicts of Interest: The authors declare no conflict of interest.

References

1. Wan, X.F.; Wang, S.; Kang, C.Z.; Lyu, C.G.; Guo, L.P.; Huang, L.Q. Chinese medicinal materials industry during the 14th Five-Year Plan period: Trends and development suggestions. *China J. Chin. Mater. Med.* **2022**, *47*, 1144–1152. [[CrossRef](#)]
2. Zhao, X.; Yue, L.; Uwaremwe, C.; Liu, Y.; Tian, Y.; Zhao, H.J.; Zhou, Q.; Zhang, Y.B.; Wang, R.Y. First report of root rot caused by the *Fusarium oxysporum* species complex on *Codonopsis pilosula* in China. *Plant Dis.* **2021**, *105*, 3742. [[CrossRef](#)] [[PubMed](#)]
3. Yu, Z.L.; Lei, M.Y.; Pu, S.C.; Xiao, Z.; Cao, H.Q.; Yang, C.Q. Fungal disease survey and pathogen identification on *Codonopsis tangshen* in Chongqing. *J. Chin. Med. Mater.* **2015**, *38*, 1119–1122.
4. Punja, Z.K.; Wan, A.; Goswami, R.S. Root rot and distortion of ginseng seedling roots caused by *Fusarium oxysporum*. *Can. J. Plant Pathol.* **2008**, *30*, 565–574. [[CrossRef](#)]
5. Di Primo, P.; Cappelli, C. Preliminary characterization of *Fusarium oxysporum* f. sp. *gladioli* causing *Fusarium* Corm rot of Saffron in Italy. *Plant Dis.* **2000**, *84*, 806. [[CrossRef](#)]

6. Gao, W.W.; Zhang, X.M.; Tian, G.L.; Jiao, X.L. Plant diseases of traditional Chinese medicines: 20 years of progress in research on understanding and management. *Plant Prot.* **2016**, *42*, 15–23.
7. Gao, F.; Ren, X.X.; Wang, M.L.; Qin, X.M. Research progress in root rot diseases of Chinese herbal medicine and control strategy by antagonistic microorganisms. *China J. Chin. Mater. Med.* **2015**, *40*, 4122–4126.
8. Raza, W.; Ling, N.; Zhang, R.F.; Huang, Q.W.; Xu, Y.C.; Shen, Q.R. Success evaluation of the biological control of *Fusarium wilt*s of cucumber, banana, and tomato since 2000 and future research strategies. *Crit. Rev. Biotechnol.* **2017**, *37*, 202–212. [[CrossRef](#)]
9. Dita, M.; Barquero, M.; Heck, D.; Mizubuti, E.S.G.; Staver, C.P. *Fusarium Wilt* of banana: Current knowledge on epidemiology and research needs toward sustainable disease management. *Front. Plant Sci.* **2018**, *9*, 1468. [[CrossRef](#)]
10. Cruz, D.R.; Leandro, L.F.S.; Munkvold, G.P. Effects of temperature and pH on *Fusarium oxysporum* and soybean seedling disease. *Plant Dis.* **2019**, *103*, 3234–3243. [[CrossRef](#)]
11. Dean, R.; Van Kan, J.A.; Pretorius, Z.A.; Hammond-Kosack, K.E.; Di Pietro, A.; Spanu, P.D.; Rudd, J.J.; Dickman, M.; Kahmann, R.; Ellis, J.; et al. The Top 10 fungal pathogens in molecular plant pathology. *Mol. Plant Pathol.* **2012**, *13*, 414–430. [[CrossRef](#)] [[PubMed](#)]
12. Staver, C.; Pemsler, D.E.; Scheerer, L.; Perez Vicente, L.; Dita, M. Ex ante assessment of returns on research investments to address the impact of *Fusarium Wilt* tropical race 4 on global banana production. *Front. Plant Sci.* **2020**, *11*, 844. [[CrossRef](#)] [[PubMed](#)]
13. Portal Gonzalez, N.; Soler, A.; Ribadeneira, C.; Solano, J.; Portieles, R.; Herrera Isla, L.; Companioni, B.; Borrás-Hidalgo, O.; Santos Bermudez, R. Phytotoxic metabolites produced by *Fusarium oxysporum* f. sp. *cubense* race 2. *Front. Microbiol.* **2021**, *12*, 629395. [[CrossRef](#)]
14. Wei, J.; Wu, B. Chemistry and bioactivities of secondary metabolites from the genus *Fusarium*. *Fitoterapia* **2020**, *146*, 104638. [[CrossRef](#)]
15. Porter, J.K.; Bacon, C.W.; Wray, E.M.; Hagler, W.M., Jr. Fusaric acid in *Fusarium moniliforme* cultures, corn, and feeds toxic to livestock and the neurochemical effects in the brain and pineal gland of rats. *Nat. Toxins* **1995**, *3*, 91–100. [[CrossRef](#)]
16. Ghazi, T.; Nagiah, S.; Dhani, S.; Chuturgoon, A.A. Fusaric acid-induced epigenetic modulation of hepatic H3K9me3 triggers apoptosis in vitro and in vivo. *Epigenomics* **2020**, *12*, 955–972. [[CrossRef](#)]
17. Onwona-Kwakye, M.; Hogarth, J.N.; Van den Brink, P.J. Environmental risk assessment of pesticides currently applied in Ghana. *Chemosphere* **2020**, *254*, 126845. [[CrossRef](#)]
18. Alshannaq, A.; Yu, J.H. Occurrence, Toxicity, and Analysis of Major Mycotoxins in Food. *Int. J. Environ. Res. Public Health* **2017**, *14*, 632. [[CrossRef](#)] [[PubMed](#)]
19. Ghosh, R.K.; Singh, N. Leaching behaviour of azoxystrobin and metabolites in soil columns. *Pest Manag. Sci.* **2009**, *65*, 1009–1014. [[CrossRef](#)]
20. Kai, K.; Wang, R.; Bi, W.; Ma, Z.; Shi, W.; Ye, Y.; Zhang, D. Chlorogenic acid induces ROS-dependent apoptosis in *Fusarium fujikuroi* and decreases the postharvest rot of cherry tomato. *World J. Microbiol. Biotechnol.* **2021**, *37*, 93. [[CrossRef](#)]
21. Marchese, A.; Barbieri, R.; Sanches-Silva, A.; Daglia, M.; Nabavi, S.F.; Jafari, N.J.; Izadi, M.; Ajami, M.; Nabavi, S.M. Antifungal and antibacterial activities of allicin: A review. *Trends Food Sci. Technol.* **2016**, *52*, 49–56. [[CrossRef](#)]
22. De Oliveira Pereira, F.; Mendes, J.M.; de Oliveira Lima, E. Investigation on mechanism of antifungal activity of eugenol against *Trichophyton rubrum*. *Med. Mycol.* **2013**, *51*, 507–513. [[CrossRef](#)] [[PubMed](#)]
23. Hua, C.Y.; Kai, K.; Wang, X.F.; Shi, W.; Zhang, D.F.; Liu, Y.S. Curcumin inhibits gray mold development in kiwifruit by targeting mitogen-activated protein kinase (MAPK) cascades in *Botrytis cinerea*. *Postharvest Biol. Technol.* **2019**, *151*, 152–159. [[CrossRef](#)]
24. Li, S.; Cheng, X.; Wang, C. A review on traditional uses, phytochemistry, pharmacology, pharmacokinetics and toxicology of the genus *Peganum*. *J. Ethnopharmacol.* **2017**, *203*, 127–162. [[CrossRef](#)]
25. Khelifi, D.; Sghaier, R.M.; Amouri, S.; Laouini, D.; Hamdi, M.; Bouajila, J. Composition and anti-oxidant, anti-cancer and anti-inflammatory activities of *Artemisia herba-alba*, *Ruta chalapensis* L. and *Peganum harmala* L. *Food Chem. Toxicol.* **2013**, *55*, 202–228. [[CrossRef](#)]
26. Cheng, X.M.; Zhao, T.; Yang, T.; Wang, C.H.; Bligh, S.W.; Wang, Z.T. HPLC fingerprints combined with principal component analysis, hierarchical cluster analysis and linear discriminant analysis for the classification and differentiation of *Peganum* sp. indigenous to China. *Phytochem. Anal.* **2010**, *21*, 279–289. [[CrossRef](#)]
27. Zhu, Z.; Zhao, S.; Wang, C. Antibacterial, antifungal, antiviral, and antiparasitic activities of *Peganum harmala* and its ingredients: A review. *Molecules* **2022**, *27*, 4161. [[CrossRef](#)]
28. Hajji, A.; Bnejdi, F.; Saadoun, M.; Ben Salem, I.; Nehdi, I.; Sbihi, H.; Alharthi, F.A.; El Bok, S.; Boughalleb-M’Hamdi, N. High reserve in delta-Tocopherol of *Peganum harmala* seeds oil and antifungal activity of oil against ten plant pathogenic fungi. *Molecules* **2020**, *25*, 4569. [[CrossRef](#)]
29. Xu, Y.Y.; Wei, J.Y.; Wei, Y.Y.; Han, P.P.; Dai, K.; Zou, X.R.; Jiang, S.; Xu, F.; Wang, H.F.; Sun, J.C.; et al. Tea tree oil controls brown rot in peaches by damaging the cell membrane of *Monilinia fructicola*. *Postharvest Biol. Technol.* **2021**, *175*, 11474. [[CrossRef](#)]
30. Ma, W.; Zhao, L.; Zhao, W.; Xie, Y. (E)-2-Hexenal, as a potential natural antifungal compound, inhibits *Aspergillus Flavus* spore germination by disrupting mitochondrial energy metabolism. *J. Agric. Food Chem.* **2019**, *67*, 1138–1145. [[CrossRef](#)]
31. Yang, Y.; Cheng, X.; Liu, W.; Chou, G.; Wang, Z.; Wang, C. Potent AChE and BChE inhibitors isolated from seeds of *Peganum harmala* Linn by a bioassay-guided fractionation. *J. Ethnopharmacol.* **2015**, *168*, 279–286. [[CrossRef](#)] [[PubMed](#)]
32. Ren, X.; Xu, Z.; Deng, R.; Huang, L.; Zheng, R.; Kong, Q. Peppermint essential oil suppresses *Geotrichum citri-aurantii* growth by destructing the cell structure, internal homeostasis, and cell cycle. *J. Agric. Food Chem.* **2021**, *69*, 7786–7797. [[CrossRef](#)] [[PubMed](#)]

33. Zhang, Q.; Liu, F.; Zeng, M.; Zhang, J.; Liu, Y.; Xin, C.; Mao, Y.; Song, Z. Antifungal activity of sodium new houttuynonate against *Aspergillus fumigatus* in vitro and in vivo. *Front. Microbiol.* **2022**, *13*, 856272. [[CrossRef](#)] [[PubMed](#)]
34. Zhang, D.; Qiang, R.; Zhou, Z.; Pan, Y.; Yu, S.; Yuan, W.; Cheng, J.; Wang, J.; Zhao, D.; Zhu, J.; et al. Biocontrol and action mechanism of *Bacillus subtilis* lipopeptides' fengycins Against *Alternaria solani* in potato as assessed by a transcriptome analysis. *Front. Microbiol.* **2022**, *13*, 861113. [[CrossRef](#)]
35. Ju, J.; Xie, Y.; Yu, H.; Guo, Y.; Cheng, Y.; Zhang, R.; Yao, W. Synergistic inhibition effect of citral and eugenol against *Aspergillus niger* and their application in bread preservation. *Food Chem.* **2020**, *310*, 125974. [[CrossRef](#)]
36. Sun, C.Q.; Peng, J.; Yang, L.B.; Jiao, Z.L.; Zhou, L.X.; Tao, R.Y.; Zhu, L.J.; Tian, Z.Q.; Huang, M.J.; Guo, G. A cecropin-4 derived peptide c18 inhibits *Candida albicans* by disturbing mitochondrial function. *Front. Microbiol.* **2022**, *13*, 872322. [[CrossRef](#)]
37. Acheuk, F.; Basiouni, S.; Shehata, A.A.; Dick, K.; Hajri, H.; Lasram, S.; Yilmaz, M.; Emekci, M.; Tsiamis, G.; Spona-Friedl, M.; et al. Status and prospects of botanical biopesticides in Europe and Mediterranean countries. *Biomolecules* **2022**, *12*, 311. [[CrossRef](#)]
38. Deng, Y.; Zhang, M.; Luo, H. Identification and antimicrobial activity of two alkaloids from traditional Chinese medicinal plant *Tinospora capillipes*. *Ind. Crops Prod.* **2012**, *37*, 298–302. [[CrossRef](#)]
39. Wang, Z.; Li, J.; Li, J.; Hui, N.; Zhou, T.; Wang, L.; Ma, Y.; Zhang, X. Identification of root rot pathogen of *Glycyrrhiza* and indoor toxicity test. *Acta Agric. Boreali-Occident. Sin.* **2013**, *22*, 98–102.
40. Mbasa, W.V.; Nene, W.A.; Kapinga, F.A.; Lilai, S.A.; Tibuhwa, D.D. Characterization and chemical management of cashew fusarium wilt disease caused by *Fusarium oxysporum* in Tanzania. *Crop. Prot.* **2021**, *139*, 105379. [[CrossRef](#)]
41. Sekhon, A.S.; Padhye, A.A.; Garg, A.K.; Ahmad, H.; Moledina, N. *In vitro* sensitivity of medically significant *Fusarium* species to various antimycotics. *Chemotherapy* **1994**, *40*, 239–244. [[CrossRef](#)] [[PubMed](#)]
42. Zhou, D.; Wang, Z.; Li, M.; Xing, M.; Xian, T.; Tu, K. Carvacrol and eugenol effectively inhibit *Rhizopus stolonifer* and control postharvest soft rot decay in peaches. *J. Appl. Microbiol.* **2018**, *124*, 166–178. [[CrossRef](#)] [[PubMed](#)]
43. Khadraoui, N.; Essid, R.; Jallouli, S.; Damergi, B.; Ben Takfa, I.; Abid, G.; Jedidi, I.; Bachali, A.; Ayed, A.; Limam, F.; et al. Antibacterial and antibiofilm activity of *Peganum harmala* seed extract against multidrug-resistant *Pseudomonas aeruginosa* pathogenic isolates and molecular mechanism of action. *Arch. Microbiol.* **2022**, *204*, 133. [[CrossRef](#)] [[PubMed](#)]
44. Olmedo, G.M.; Cerioni, L.; Gonzalez, M.M.; Cabrerizo, F.M.; Volentini, S.I.; Rapisarda, V.A. UVA photoactivation of harmol enhances its antifungal activity against the phytopathogens *Penicillium digitatum* and *Botrytis cinerea*. *Front. Microbiol.* **2017**, *8*, 347. [[CrossRef](#)] [[PubMed](#)]
45. Chen, Y.; Dangol, S.; Wang, J.; Jwa, N.S. Focal accumulation of ros can block *Pyricularia Oryzae* effector BAS4-expression and prevent infection in rice. *Int. J. Mol. Sci.* **2020**, *21*, 6196. [[CrossRef](#)] [[PubMed](#)]
46. Hwang, J.H.; Hwang, I.S.; Liu, Q.H.; Woo, E.R.; Lee, D.G. (+)-Medioresinol leads to intracellular ROS accumulation and mitochondria-mediated apoptotic cell death in *Candida albicans*. *Biochimie* **2012**, *94*, 1784–1793. [[CrossRef](#)]
47. Hirayama, T.; Miyazaki, T.; Sumiyoshi, M.; Ashizawa, N.; Takazono, T.; Yamamoto, K.; Imamura, Y.; Izumikawa, K.; Yanagihara, K.; Kohno, S.; et al. ERG3-encoding sterol C5,6-Desaturase In *Candida albicans* is required for virulence in an enterically infected invasive *Candidiasis* mouse model. *Pathogens* **2020**, *10*, 23. [[CrossRef](#)]
48. Liu, J.; Chai, X.; Guo, T.; Wu, J.; Yang, P.; Luo, Y.; Zhao, H.; Zhao, W.; Nkechi, O.; Dong, J.; et al. Disruption of the ergosterol biosynthetic pathway results in increased membrane permeability, causing overproduction and secretion of extracellular monascus pigments in submerged fermentation. *J. Agric. Food Chem.* **2019**, *67*, 13673–13683. [[CrossRef](#)]
49. OuYang, Q.; Liu, Y.; Oketch, O.R.; Zhang, M.; Shao, X.; Tao, N. Citronellal exerts its antifungal activity by targeting ergosterol biosynthesis in *Penicillium digitatum*. *J. Fungi* **2021**, *7*, 432. [[CrossRef](#)]
50. Zhang, C.; Zhao, J.; Famous, E.; Pan, S.; Peng, X.; Tian, J. Antioxidant, hepatoprotective and antifungal activities of black pepper (*Piper nigrum* L.) essential oil. *Food Chem.* **2021**, *346*, 128845. [[CrossRef](#)]